Computerized Medical Imaging and Graphics 35 (2011) 472–480

Contents lists available at ScienceDirect

Computerized Medical Imaging and Graphics

journal homepage: www.elsevier.com/locate/compmedimag

Automated selection of major arteries and veins for measurement of arteriolar-to-venular diameter ratio on retinal fundus images

Chisako Muramatsu [a,*], Yuji Hatanaka [b,1], Tatsuhiko Iwase [a,2], Takeshi Hara [a,3], Hiroshi Fujita [a,3]

[a] Department of Intelligent Image Information, Graduate School of Medicine, Gifu University, 1-1 Yanagido, Gifu 501-1194, Japan
[b] Department of Electronic Systems Engineering, School of Engineering, The University of Shiga Prefecture, 2500 Hassakacho, Hikone, Shiga 522-8533, Japan

ARTICLE INFO

Article history:
Received 6 October 2010
Received in revised form
27 December 2010
Accepted 16 March 2011

Keywords:
Arteriolar narrowing
Arteriolar-to-venular diameter ratio (AVR)
Computerized measurement
Retinal fundus images
Hypertensive retinopathy

ABSTRACT

An automated method for measurement of arteriolar-to-venular diameter ratio (AVR) is presented. The method includes optic disc segmentation for the determination of the AVR measurement zone, retinal vessel segmentation, vessel classification into arteries and veins, selection of major vessel pairs, and measurement of AVRs. The sensitivity for the major vessels in the measurement zone was 87%, while 93% of them were classified correctly into arteries or veins. In 36 out of 40 vessel pairs, at least parts of the paired vessels were correctly identified. Although the average error in the AVRs with respect to those based on the manual vessel segmentation results was 0.11, the average error in vessel diameter was less than 1 pixel. The proposed method may be useful for objective evaluation of AVRs and has a potential for detecting focal arteriolar narrowing on macula-centered screening fundus images.

1. Introduction

Retinal fundus photographs permit noninvasive visualization of the retinal vasculature, which can indicate health conditions, such as diabetes and high blood pressure. Previous studies have reported the association of retinal microvascular abnormalities with cardiovascular and cerebrovascular diseases [1,2]. Although the accessibility of retinal fundus photographs makes this examination suitable for screening these diseases, a large number of examinations will result in an increased burden for ophthalmologists. Computerized analysis of retinal fundus images can potentially reduce ophthalmologists' workload and improve diagnostic efficiency.

One of the hypertension-associated findings in retinal fundus images is arteriolar narrowing, which can be assessed by arteriolar-to-venular diameter ratios (AVR). In Japan, it is often measured in pairs of large vessels running side by side at a certain distance from the optic nerve head towards the temporal side in macula-centered photographs. In the U.S., AVR is commonly determined using the six largest arteries and veins on retinal fundus images centered at the optic disc, as suggested by Knudtson et al. [3]. However, in screening examinations, the fundus images obtained are usually macula-centered for screening for various diseases in the larger retinal area. Therefore, it may be more reliable to use temporal vessels for the AVR measurement in such images. The regions in which AVRs are measured, referred to as the measurement zones in this study, are defined as the regions between the half-disc and one-disc diameters from the optic disc margin in the U.S. [4] and between the quarter-disc and one-disc diameters from the optic disc margin in Japan. Despite the existence of such guidelines, the AVR is seldom measured systematically or quantitatively, making consistent and longitudinal evaluations difficult. An automated measurement of AVR can facilitate ophthalmologists' evaluation of retinal fundus images.

Numerous studies, including our own [5], have been conducted to develop an automated segmentation of retinal vessels on retinal fundus images. Many of these studies utilized the public database, Digital Retinal Images for Vessel Extraction (DRIVE) [6], and these are listed in [7]. Several groups have investigated computerized quantification of vessel diameters and measurement of AVR. Gao et al. [8] proposed a semi-automated method to estimate vessel diameters and angular geometry at bifurcations. By fitting Gaussian functions to a vessel profile, calculation of the diameters of arteries for evaluation of diameter alterations possibly associated with hypertension is possible. A semi-automated method introduced by Pedersen et al. [9] obtains a series of profiles between two

* Corresponding author. Tel.: +81 58 230 6519; fax: +81 58 230 6514.
E-mail addresses: chisa@fjt.info.gifu-u.ac.jp (C. Muramatsu), hatanaka.y@usp.ac.jp (Y. Hatanaka), tatsuhiko.iwase@ntt-neo.co.jp (T. Iwase), hara@info.gifu-u.ac.jp (T. Hara), fujita@fjt.info.gifu-u.ac.jp (H. Fujita).
[1] Tel.: +81 749 28 9556; fax: +81 749 28 9576.
[2] Present address: Strategy Planning Department, NTT-Neomeit Chugoku Branch Office, 3-12-11 Ujinakanda, Minami-ku, Hiroshima 734-0004, Japan.
Tel.: +81 82 505 4778; fax: +81 82 250 7465.
[3] Tel.: +81 58 230 6519; fax: +81 58 230 6514.

0895-6111/$ – see front matter © 2011 Elsevier Ltd. All rights reserved.
doi:10.1016/j.compmedimag.2011.03.002

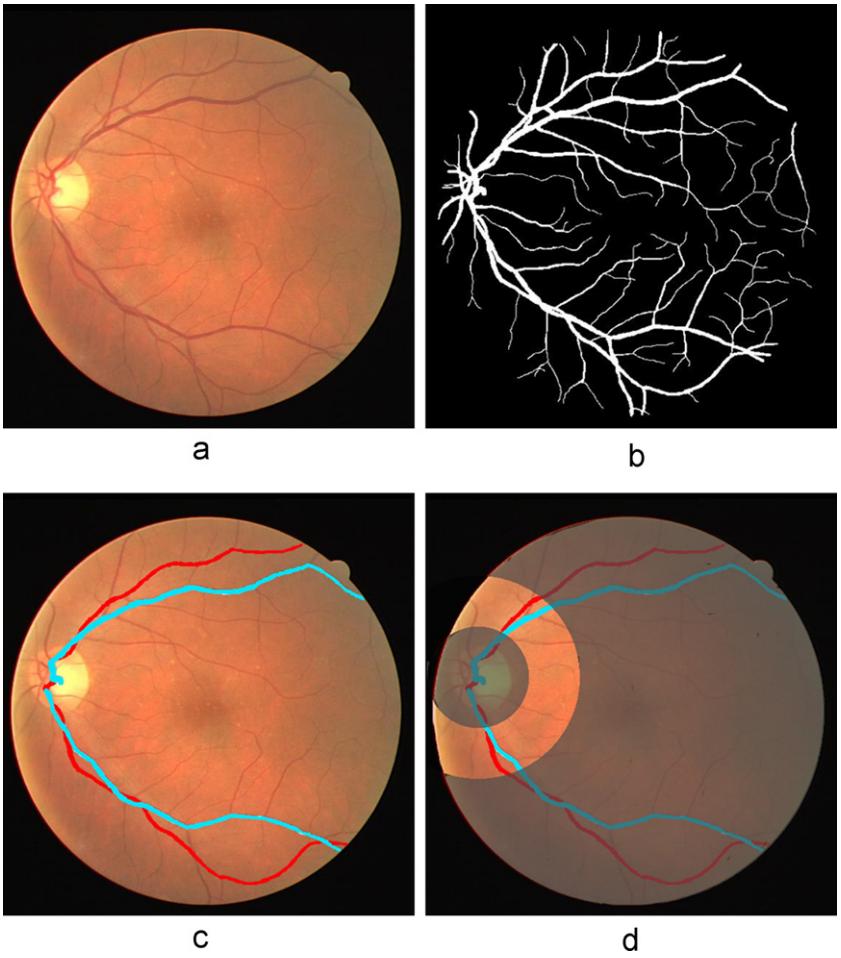

Fig. 1. (a) Original image. (b) Manual vessel segmentation result (reference standard) provided in DRIVE database. (c) Gold standard of major arteries and veins. (d) AVR measurement zone.

manually defined points on an artery. The diameters are estimated by the full-width at half maximum of the profiles for detection of focal arteriolar narrowing. Hubbard et al. [4,10] developed a semi-automated method for measuring and summarizing arteriolar and venular diameters, which was employed in a large cohort study called the Atherosclerosis Risk in Communities (ARIC) Study. In this method, a grader identifies arteries and veins, selects segments within the measurement zone for calculation of diameters, and accepts or adjusts the measurements made by the software. Another semi-automated method that requires the manual identification of pairs of vessels was introduced by Patker et al. [11]. On the basis of the manual inputs, the software automatically detects the edges of vessel walls and calculates the vessel diameters. This group reported good interobserver reproducibility by users of this system.

An automated method with the option of manual correction for AVR estimation was proposed by Tramontan et al. [12,13]. In their system, retinal vessels are extracted by vessel tracing, the optic disc is located on the basis of the vessel network, the extracted arteries and veins are discriminated by the feature characterizing the central reflex, and the AVR is estimated using vessels with diameters greater than 45 μm. Vessel segmentation and classification can be corrected manually if needed. A good correlation between the AVRs determined by the proposed method and manual measurement was reported by this group. The AVR measurement method proposed by Nam et al. [14] is based on the circular intensity profile. The optic disc is first detected using the red channel of the RGB color image, and the intensity profile of the green channel is obtained along the perimeter of a circle whose radius is equal to the optic disc's diameter and is centered on the optic disc. The valleys in the profile are considered as vessels, which are classified into arteries and veins according to their shapes. Vessels larger than 7 pixels are used for the calculation of AVR. Niemeijer et al. [15] proposed a fully automated method for the determination of AVR. They detect the location of the optic disc, determine the region of interest (ROI) for AVR measurements, classify the vessels into arteries and veins, and measure the AVR. For classification of the vessels, they tested the k-nearest neighbor, support vector machine, linear discriminant classifier and quadratic discriminant classifier and found that the linear classifier worked best for their dataset. This study most closely resembles our current study.

In this study, we propose a fully automated AVR measurement method composed of vessel extraction, optic disc detection, vessel classification, vessel selection, and diameter measurement. The method selects two pairs of major vessels in the upper and lower temporal regions. Unlike averaging the diameters of several vessels, the selection of a pair of vessels may potentially detect focal thinning.

2. Image database

The retinal fundus images used in this study were obtained from the DRIVE database, a database of images acquired in a diabetic retinopathy-screening program in the Netherlands [6,7]. Although the images may include some pathological lesions, this information is not available to us. Because we are unable to determine

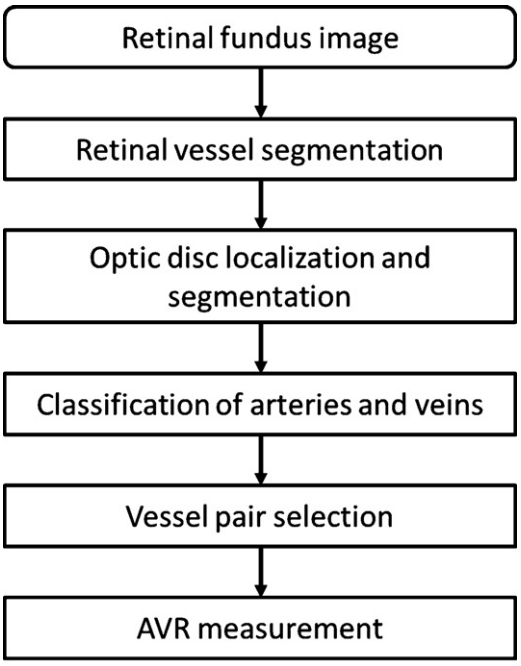

Fig. 2. Flowchart of the overall scheme for AVR measurement.

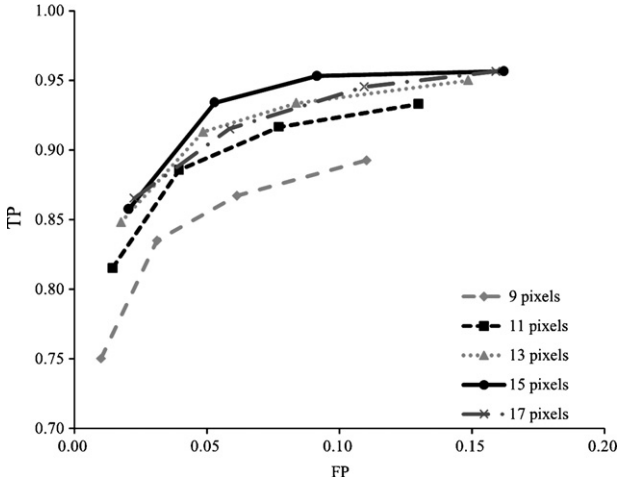

Fig. 3. The relationship between true positive fraction and false positive fraction for extracting major retinal vessels in the training cases with the top-hat filters of different diameters.

whether the cases include arteriolar narrowing, the evaluation of our scheme is based on the measurement of AVR rather than detection of arteriolar narrowing. The DRIVE database consists of 20 training and 20 test cases. In this study, the training cases are used for developing the scheme and determining the parameters, whereas the test cases are employed without adjusting the parameters, for evaluating the robustness of the method.

The images were saved in JPEG format with 565×584 pixels. For each image, the manual segmentation result of the vasculature is provided, which is considered the reference standard for the vessels. In this study, we focus on extracting and selecting two pairs of major vessels to measure AVR. These four vessels are selected from the manual segmentation result and classified into arteries and veins by an ophthalmologist, as shown in Fig. 1. These are employed as the gold standard for major arteries and veins. On the basis of these gold standard images, the gold standard vessel diameters are automatically computed in the measurement zone. For this purpose, the optic disc centers and diameters are manually identified. Vessels are first reduced to single-pixel-wide lines using a morphological thinning algorithm [16]. At each of the retained pixels, called centerline pixels, the shortest path inside the original vessel through the centerline pixel is determined as the diameter at that point. The ratio of the average diameters of the paired artery and vein is considered the gold standard AVR.

3. Methods

The proposed automated scheme for determining AVR consists of segmentation of retinal vessel, localization and segmentation of the optic disc to identify the measurement zone, classification of vessels into arteries and veins, selection of vessels for measurement, and measurement of AVR. The flowchart of the overall scheme is shown in Fig. 2.

3.1. Vessel segmentation

Retinal blood vessels are extracted using a previously developed method that employs a combination of top-hat transformation (THT) and double-ring filtering (DRF) techniques [5,17]. The THT is applied to the green channel of the color images, which generally exhibits the highest contrast for retinal vessels. The filter element is set to be a circle with a diameter of 15 pixels based on the sensitivity and specificity on the training cases. The relationship between sensitivity and false positive fraction (1 − specificity) for extracting the major vessels with filters of different diameters is shown in Fig. 3. Because the diameters of the large vessels are about 11 pixels, the curve for the 9-pixel diameter filter is apparently lower. The result indicates that filter with a 15-pixel diameter provide the optimal sensitivity/specificity pair. Similarly, the DRF is applied to the green channel images. The DRF consists of inner and outer square regions with widths of 3 and 13 pixels, respectively. The pixel of interest is replaced by the difference in the average pixel values in the inner square and the surrounding region. The outputs from the THT and DRF are summed, and the vessel regions are determined by applying a threshold. The threshold is set to be 15% based on the average percentage of the gold standard pixels in the training cases, which is about 12.5%. In order to remove small vessels that are not used for the measurement of AVR, the vessels with the diameter less than three pixels are removed.

The extracted retinal vessels are partitioned into vessel segments by identifying the vessel crossings and bifurcations. To identify the crossings and bifurcation, the centerline pixels of the vessels are determined; these are also used in the classification of vessel segments into arteries and veins. If a centerline pixel has more than two neighboring pixels corresponding to centerline pixels, it is considered that either a vessel crossing or a bifurcation is present around that pixel. In such cases, a search for the shortest paths to the non-vessel pixels, in the direction between these neighbor pixels, is performed. By connecting these ends and removing the pixels inside, the vessels are disconnected.

3.2. Optic disc segmentation

Optic disc locations and approximate disc diameters are determined using an active contour method to determine the AVR measurement zone. The basic scheme for the segmentation of optic disc is described in detail elsewhere [18]. Briefly, an approximate location of the optic disc is identified using the p-tile thresholding method on the red channel image, and an ROI is extracted at the identified location. On the basis of the edges detected by the Canny edge detector, an active contour model is employed for determining the disc contour.

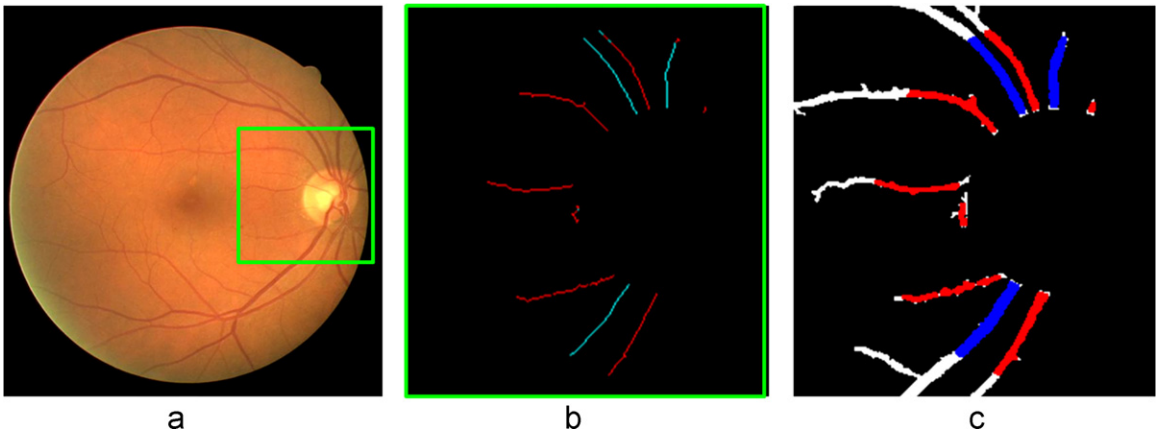

Fig. 4. Classification of vessels. (a) Original image. (b) Classification result for the centerline pixels into those belonging to arteries (red) or veins (blue). (c) Classification result for the vessel segments by the majority rule. (For interpretation of the references to color in this figure legend, the reader is referred to the web version of the article.)

In our previous study [18], most images were obtained using a stereo camera with a 27° field of view (FOV) and a 1600 × 1200 pixel matrix. Furthermore, the overall image brightness and the color of the retina were somewhat different from those of the DRIVE cases, which may be due to differences in the camera systems, the condition of individual patients, and the demography of the patients. Therefore, the optic disc detection algorithm was retrained using the training cases. For identification of approximate disc locations, instead of applying the p-tile thresholding method to the red channel images, the color channel is automatically selected in each case depending on the brightness of the image. As a result, for bright images in which the pixel values in the red channel are saturated, the green channel is employed in the thresholding method. Because the DRIVE cases were obtained with a 45° FOV and 565 × 584 pixels, the size of the ROI is set to 200 × 200 pixels, and the threshold value is set to 4500 pixels (11.25%). In this study, our purpose is to determine the disc diameter to identify the measurement zone. Therefore, the determined disc contour is fitted by an ellipse, and the length of the major axis is used as the diameter of the disc. This method failed to detect the correct location of the disc in just one training case, which had a large pathology region. However, considering that such cases are relatively uncommon in general screening, the method was applied as is to the test cases.

3.3. Retinal vessel classification into arteries and veins

Each centerline pixel of the vessel segments in the measurement zone is classified into those belonging to an artery or vein using a linear discriminant classifier. Ophthalmologists often distinguish arteries and veins based on their color and thickness. In this study, we determine six features, three of which correspond to the original color components (red, green, and blue), and three correspond to the contrast in the three color channels. The contrast is defined as the difference in average pixel values in a 5 × 5 pixel region around the pixel of interest inside the vessel, and in a 10 × 10 pixel region around the pixel of interest outside the vessel. Using the stepwise feature selection, one feature—the contrast in blue component—is excluded, and the remaining five features are employed for training the classifier. For this training, the centerline pixels of the gold standard major vessels are used, and the result of the resubstitution test showed a classification accuracy of 92.8%. On the basis of the result for the centerline pixels, each vessel segment is classified into an artery or a vein by selecting a majority group as shown in Fig. 4.

3.4. Major vessel pair selection

At this point, vessels that would not be used for the measurement of AVR are still present. The potential vessel segments that are considered as parts of the paired major vessels in the upper and lower temporal regions are selected by a series of rules described below. First, small vessel segments with areas less than 50 pixels are removed. In this study, our target is to select major vessels running from the optic disc to the upper and lower temporal regions. Therefore, the vessel segments on the nasal side and those corresponding to the side branches are dismissed on the basis of the vessel direction.

To determine the direction of the vessels, a determination of whether an image is of the right or left eye is made. The DRIVE database includes some images in which the FOV are not centered at the macula. Therefore, the distinction between the right and the left eye is made on the basis of whether an image is macula-centered and on the basis of the brightness inside the optic disc. The average pixel value in a 50 × 50 pixel region around the center of the FOV is compared with that of the surrounding squared-frame region, and in these regions, the sizes of the outer and inner squares are 150 and 100 pixels, respectively. The sizes of these regions are determined empirically. If the center region is darker than the outer region, the image is macula-centered. The image is considered as that of the right or left eye, when the optic disc is located at the right or left side, respectively, of the FOV. If an image is not macula-centered, it is considered as the left and right eye, respectively.

In the second method to determine whether the image is of the right or left eye, the average pixel values in 60 × 30 pixel regions on the right and left sides of an optic disc center are compared. The large vessels coming into an optic disc are usually gathered at the nasal side of the disc, and therefore, the pixel values inside the optic disc tend to be higher on the temporal side than on the nasal side [19]. If the average pixel value in the right side is higher than that in the left side, the image is considered as the left eye, and vice versa. When the results from the two methods disagree, the result of the brightness inside the optic disc is employed if the difference in the average pixel values is larger than 30, whereas the result of the macula analysis is employed if the difference is small. For both methods, the green channel images are used.

The direction of the vessel segments is determined with respect to the horizontal line from the optic disc to the nasal direction as the zero degree. The vessel segments above and below the optic disc center with directions from 80° to 180° and from −80° to −180°, respectively, are retained, and the other segments are removed

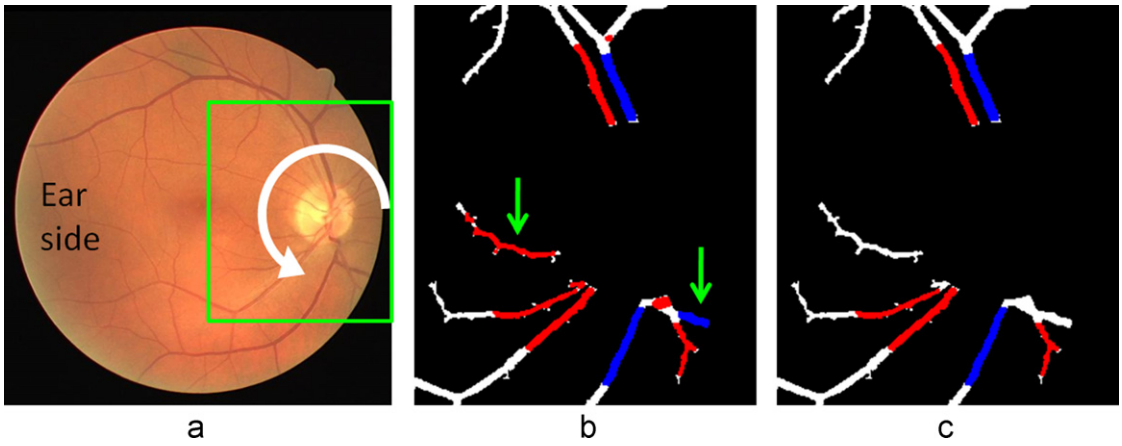

Fig. 5. Vessel selection by direction analysis. (a) Original image. Green arrow shows the radial angle direction from the nose side (0°) to the ear side (180°). (b) Vessel segments remained before the direction analysis. Green arrows specify the segments that were removed based on their direction. (c) Vessel segments remained after the direction analysis. (For interpretation of the references to color in this figure legend, the reader is referred to the web version of the article.)

from the candidates. These angle thresholds are determined on the basis of the gold standard major vessels in the training cases. Fig. 5 shows the retained candidate vessels before and after the direction analysis. It can be seen that segments indicated with arrows are removed from the candidate vessels for AVR measurement.

Of the remaining segments, those that are considered as parts of the paired major arteries and veins are selected in each of the upper and lower regions at concentric circles, with radii of every five pixels in the measurement zone. At each increment, the rules specified in Fig. 6 are applied. Both vessels are selected if there are only two vessels corresponding to an artery and a vein. If, however, two arteries (or two veins) remain, the vessel with the lower fraction of artery (or vein) pixels, according to the centerline pixel analysis, is switched to a vein (or an artery), only if the fraction was lower than 70%, and these two vessels are selected as the pair. When there are more than two candidate vessels, the three vessels

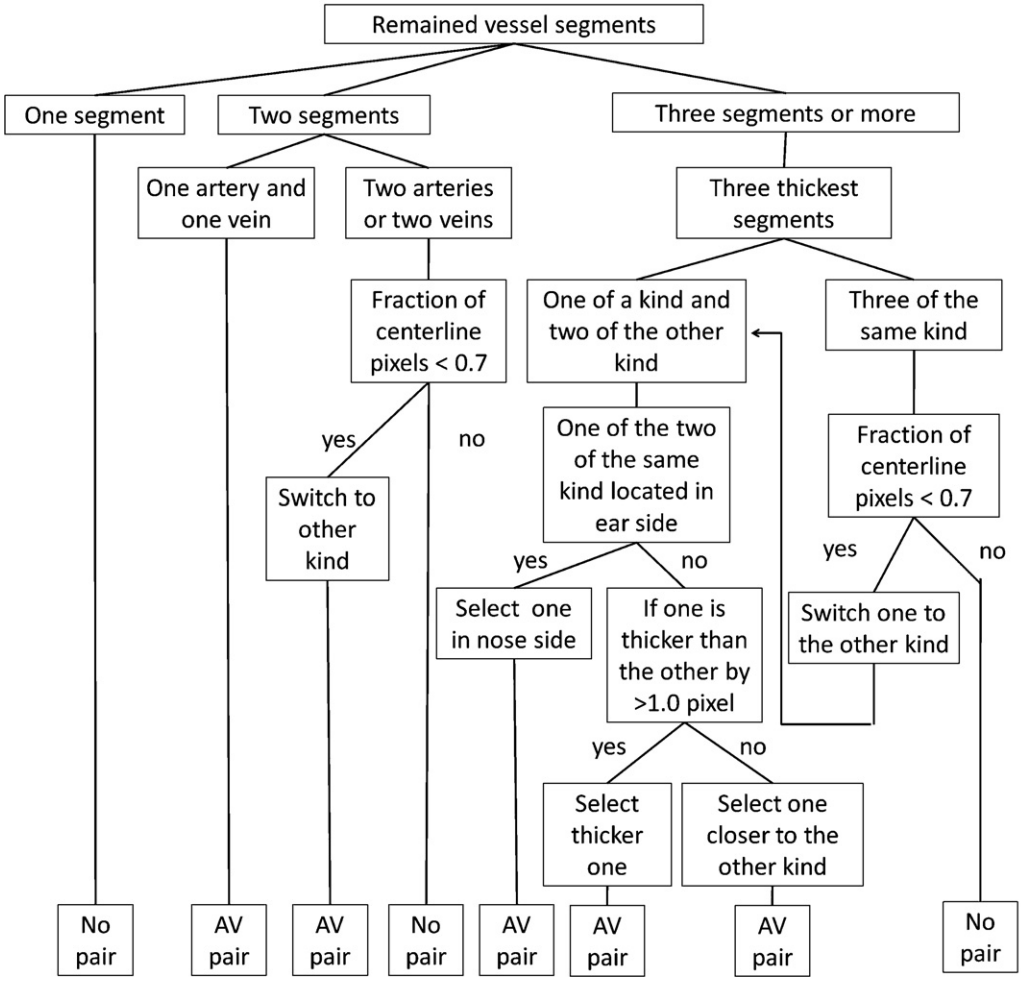

Fig. 6. Vessel selection rules. Different rules were applied depending on the number of remained vessel segments.

with the largest diameters are considered. If three vessels include both an artery and a vein, e.g., one artery and two veins, one of the two veins is paired with the artery by the following rule: (1) if one seems to be located on the nasal side with respect to the optic disc center, the other vessel is selected; (2) if both are located on the temporal side, the vessel with an average diameter larger than the other by more than one pixel is selected; and (3) if the diameters of the two vessels are comparable, the vessel that is closest to the artery is selected. The same rule is applied when the three vessels include one vein and two arteries. When the three vessels are of the same kind, one of them is switched to the other kind in the same manner as above, and one of the remaining two vessels is selected as explained above. If there is only one candidate vessel, or if a vessel could not be switched, it is considered that no matched pair exists.

3.5. AVR measurement

The diameters of the vessels are determined by the length of the shortest path through the centerline pixels inside the vessel region. At each vessel selection increment, the diameters of the artery and the vein are determined by averaging the diameters of the centerline pixels that are within the distance of 3 pixels from the point of interest, if a pair of major vessel exists and if the centerline pixels belong to the selected artery or vein. The AVRs are determined at these points which are then averaged for the upper and lower pairs. The results are compared with the gold standard AVRs.

4. Results

4.1. Vessel segmentation

The retinal vessel regions were extracted in the test cases by thresholding the averaged outputs from THT and DRF techniques. The sensitivity of extracting major vessels and the specificity of detecting non-vessels in the measurement zone were 87% and 97%, respectively, which were equivalent to those for the training cases (87% and 96%, respectively). In most cases, the major vessels were adequately extracted. However, it was generally more difficult to detect arteries than veins due to their lower contrast. The FOVs were not centered at the macula in two test images. Although the sensitivities for two of three cases in which FOVs were not centered at the macula in the training set were somewhat lower than the other cases, there was no apparent difference in the sensitivities due to FOV in the test set. Some of the vessel segmentation results are shown in Fig. 7.

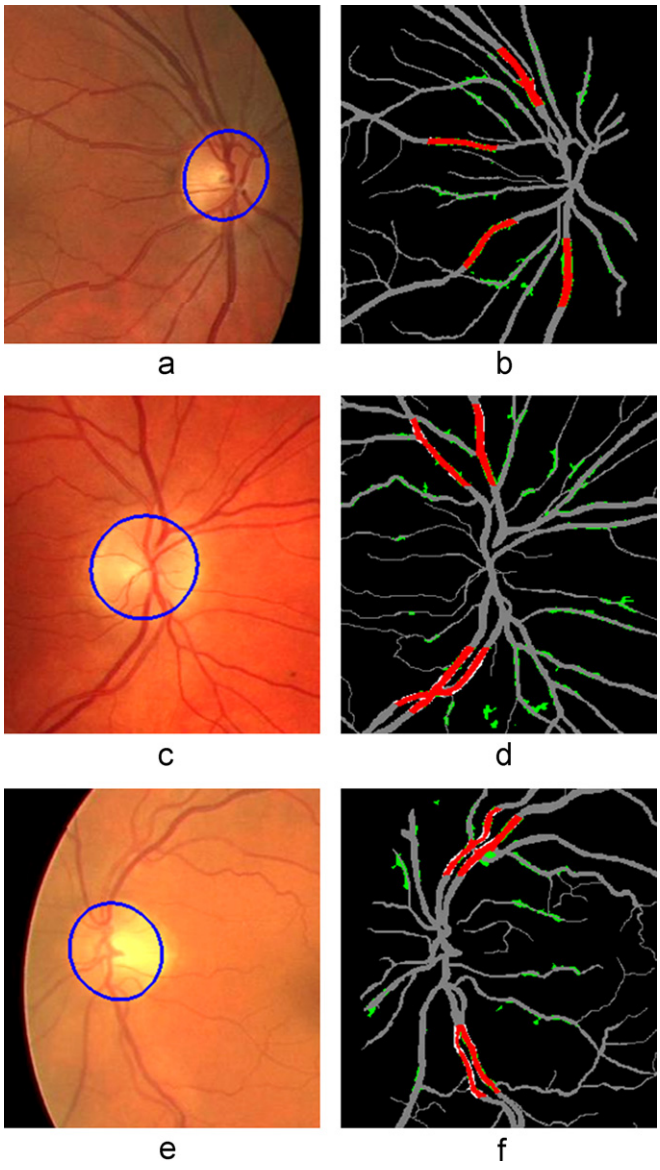

Fig. 7. Results of major vessel segmentation in measurement zone for the test cases. (a, c, and e) Original images with optic disc segmentation results. (b, d, and f) Segmentation results for (a, c, and e). Red pixels indicate the true detection, green pixels indicate the false detection, and white pixels indicate no (false negative) detection. Gray pixels indicate the rest of the vessels that were not counted. (For interpretation of the references to color in this figure legend, the reader is referred to the web version of the article.)

4.2. Optic disc segmentation

In this study, the optic disc was segmented for the purpose of determining the AVR measurement zone. The segmentation results for some cases are shown in Fig. 6. There was no firm gold standard for the optic disc regions outlined by ophthalmologists for these cases. Compared with the manually identified centers by one of the co-authors (T.I.), the average shift in the x and y directions were 5.5 and 4.2 pixels, respectively, with a distance of 7.7 pixels. In 16 of 20 cases, the distance was within 10 pixels. The average difference in diameters was 7.0 pixels (8.2%), and the difference was within 10 pixels in 17 out of 20 cases. This result suggested that the positions where AVRs would be measured were slightly different from those desired.

4.3. Vessel classification

By use of the classifier trained with five image features in the training cases, the centerline pixels of the candidate vessels in the test cases were classified into those belonging to arteries and veins. The classification accuracy of the centerline pixels of the detected major vessels was 92.8%, which was equivalent to that for the training cases (result of the resubstitution test). On average, the classification was more accurate for veins (96.0%) than for arteries (90.5%). However, in half of the cases, all the pixels belonging to the veins were classified correctly, whereas in 8 out of 20 cases, all of the artery pixels were classified correctly. In four cases, the classification was perfect for the major vessels.

On the basis of the result for these centerline pixels, the vessel segments in the measurement zone were classified as to whether they were parts of arteries or veins. By the majority rule, 54 and 74 segments were classified correctly as arteries and veins, respectively, whereas seven and two segments that were parts of major arteries and veins, respectively, were misclassified. Note that small segments with areas less than 20 pixels were not

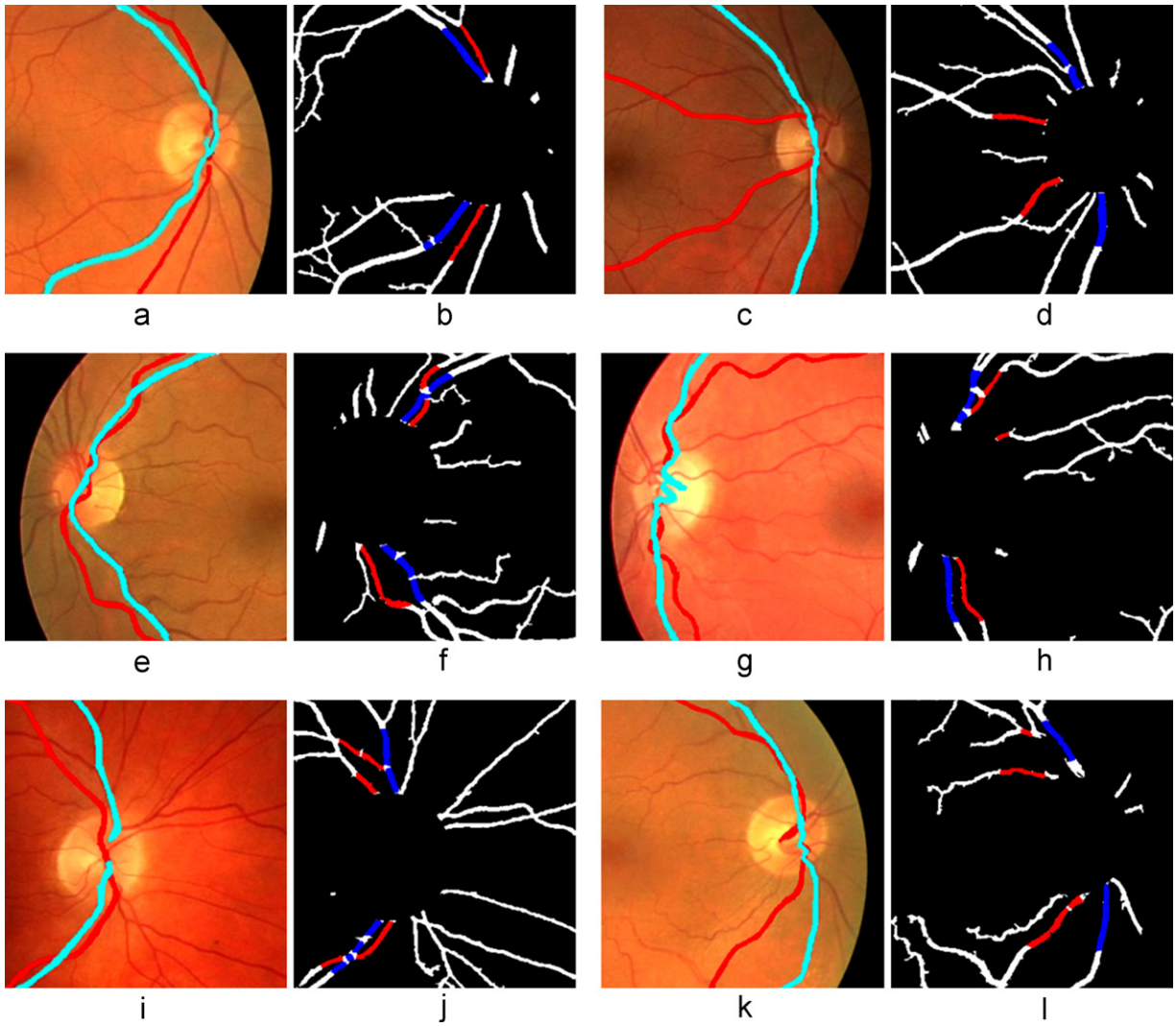

Fig. 8. Vessel selection results. (a, c, e, g, i and k) Original images with the gold standard. (b, d, f, h, j and l) Selected paired arteries (red) and veins (blue) for (a, c, e, g, i and k). Correct vessel selection in upper and lower pairs (b, d and f). Correct selection in lower pair and partially correct selection in upper pair (h and j). Correct selection in upper pair and wrong selection in upper pair due to missegmentation of artery (l). (For interpretation of the references to color in this figure legend, the reader is referred to the web version of the article.)

counted, and other segments that were part of major vessels but missed in the vessel segmentation process were not included in this analysis. Some of the misclassified segments were later switched to the correct classification during the vessel selection process.

4.4. Vessel selection

At distances of every five pixels in the measurement zone, pairs of major arteries and veins were selected for measurement of AVR. In 29 out of 40 pairs, the paired vessels were predominantly identified and selected correctly (both vessels were correctly selected in more than 70% of the part, and one of the pair was misselected in the remaining part). In some cases, when the major vessels were disconnected due to vessel crossings or bifurcations, other vessel segments were selected instead. In 7 out of the remaining 11 pairs, a proportion of the paired vessels was misselected (both vessels were correctly selected in more than 30% of the part, and one of the pair was misselected in the rest). The remaining four pairs were misselected, mostly because the major arteries were not detected due to their low contrast. Fig. 8 shows the results of the correct and incorrect selections.

4.5. AVR measurement

From the selected pairs of vessels, the average AVRs were determined. The measured AVRs ranged from 0.44 to 0.98, whereas the gold standard AVRs ranged from 0.49 to 1.12. The average error in AVRs was 0.11, whereas errors for the upper and lower pairs were 0.13 and 0.10, respectively, indicating there was no location effect ($p = 0.5$ by the t-test). Excluding the 4 and 11 pairs, in which the majority and minority, respectively, of major vessels were incorrectly selected, the average errors in AVRs were both 0.11. These results indicate that incorrect selection of the major vessels could not completely account for the measurement errors. The average errors in the measured diameters were 0.71 and 0.70 pixels for the arteries and veins, respectively.

5. Discussion

A computerized scheme for the fully automated measurement of AVRs in retinal fundus images is investigated. The proposed scheme is trained and refined using the training dataset and evaluated on the test dataset in the DRIVE database.

The retinal blood vessels are segmented by a combination of two methods, i.e., the THT and DRF. These techniques have advantages and disadvantages [17]. While vessel walls extracted by the THT tend to be uneven, optic disc edges are often misdetected as vessels by the DRF. In general, the THT provides higher sensitivities with higher false positive rates than the DRF. By combining the two methods, the high sensitivity obtained by THT is retained while taking advantage of the lower false positive rate achieved by the DRF. There are many research groups investigating segmentation methods for the retinal blood vessels [7]. The results cannot be compared directly because our goal in this study is to extract large vessels to be used for the measurement of AVR, and we do not focus on extracting small vessels as others did. The equivalent results for the training and test cases suggest that comparable results can be expected in images with similar image quality. However, the sensitivity needs to be improved, especially for the arteries. The image contrasts for some of the arteries are very low, making it difficult to extract them concomitantly with veins. A new approach may be needed for accurate segmentation of the arteries.

The optic discs are automatically segmented for determining the AVR measurement zone. When the disc segmentation is not accurate, the region where AVRs are measured would differ from that used for establishing the gold standard. As a result, the measured diameters could potentially become larger or smaller depending on its location with respect to the "true" optic disc center. In this study, the identified centers are shifted on about 8 pixels on average, and the diameters are about 7 pixels larger or smaller. To examine the effect of the automated segmentation of the optic disc, AVRs are measured using the manually determined disc centers and diameters. By use of the manual data, the location of the AVR measurement was generally, but slightly more accurate, except for one pair, in which the correct artery was not selected because it was not included in the candidates of the three largest vessels because of a slight decrease in the average diameter. The average errors in AVRs for 35 and 29 pairs corresponding to the exclusion of cases with the major and partial misselection were 0.12 and 0.11, respectively. These results indicate that the effect of the slight shift of the measurement zone on the AVR is small.

In this study, we set the measurement zone as the region between a quarter-disc to a one-disc diameter from the optic disc margin according to Japanese guidelines. In other countries, the region between a half-disc to a one-disc diameter from the optic disc margin is used. With this criterion, the average errors in AVRs were 0.14 and 0.13, which were slightly higher than the original results. The probable reason for this might be the limited measurement data. In clinical practice, ophthalmologists probably select one or several points for the measurement of AVRs. It is likely that they avoid regions where vessels cross or bifurcate, and where the contrast of vessels is low. Therefore, in future, the measurement zone for each case should be selectively determined.

Using the linear classifier, most vessel segments are classified correctly into arteries and veins. The use of other types of classifiers may improve the classification accuracy. In this study, the color information and the contrast are used for classifying the vessels. Other groups have used the red contrast [12,13], features characterizing the vessels' intensity profiles [14], and features based on the hue, saturation, and intensity [15]. Although the number of features and definitions are different, the basic idea of differentiating arteries and veins based on their difference in intensity and the presence of central reflex in arteries is similar.

In this study, paired major vessels are selected for the measurement of AVRs according to the guideline. Other groups selected several large vessels and employed the average diameters. Selection of specific pairs may allow computerized schemes to be more sensitive to localized arteriolar narrowing. On the other hand, vessels selection can be simplified in the other method. When a system is expected to suggest the locations of suspected narrowing, vessels need to be paired. However, when a system is used for initial screening of cases, i.e., merely picking up cases with potential narrowing, or detecting entirely affected cases, averaging the diameters of several vessels may reduce the effect of missegmentation and misselection of vessels. The number of measured vessels can be varied depending on the ophthalmologists' expectation.

Because the vessels are disconnected at vessel crossings and bifurcations, the paired vessels are selected at distances of every 5 pixels in the radial direction with respect to the optic disc center. At present, the segments could not be reconnected accurately because vessel crossings are not optimally differentiated from bifurcations. In future, when vessels can be appropriately reconnected, vessel classification, selection, and measurement may be improved. Although AVRs are measured at a distance of every 5 pixels, they are averaged for the pair for evaluation. Because the measurement points in testing differed from those used in establishing the gold standard, it is difficult to compare each measurement. In this study, we evaluated our automated measurement scheme in the absence of the gold standard for arteriolar narrowing. The scheme should be evaluated with abnormal cases with gold standard locations of arteriolar narrowing in the future.

The measured AVRs are compared with the gold standard AVRs determined using the manual segmentation results provided in the DRIVE database. The average error in AVRs is 0.11. There could be several reasons for the measurement errors: (1) errors in vessel segmentation results, especially for arteries with low contrast; (2) exclusion of regions of vessel crossings and bifurcation for the measurements; (3) errors in optic disc segmentation that result in differences in the AVR measurement zone; and (4) misselection of paired major vessels. Although the average error may seem large, the average errors in vessel diameters were less than 1 pixel for both arteries and veins. The low spatial resolution of the images made the accurate measurement and meaningful evaluation difficult. In the future, our computerized scheme must be evaluated with images acquired using a newer camera with higher spatial resolution.

6. Conclusion

An automated AVR measurement method is proposed. Retinal blood vessels were segmented, classified into arteries or veins, and two pairs of major arteries and veins were selected for the measurement of AVRs. In 36 out of 40 pairs, at least parts of the major vessel pairs were selected correctly. Although the average error in the AVRs was 0.11, the average errors in measured diameters were less than 1 pixel. The proposed scheme needs to be evaluated with high-resolution images including the images from patients exhibiting arteriolar narrowing.

Acknowledgments

Authors thank Tetsuya Yamamoto, M.D., and Akira Sawada, M.D., for their contribution in this study.

References

[1] Wong TY, Klein R, Couper DJ, Cooper LS, Shahar E, Hubbard HD, et al. Retinal microvascular abnormalities and incident stroke: the Atherosclerosis Risk in Communities Study. Lancet 2001;358:1134–40.
[2] McClintic BR, McClintic JI, Bisognano JD, Block RC. The relationship between retinal microvascular abnormalities and coronary heart disease: a review. Am J Med 2010;123:374.e1–7.
[3] Knudtson MD, Lee KE, Hubbard LD, Wong TY, Klein R, Klein BEK. Revised formulas for summarizing retinal vessel diameters. Curr Eye Res 2003;27:143–9.
[4] Hubbard LD, Brothers RJ, King WN, Clegg LX, Klein R, Cooper LS, et al. Methods for evaluation of retinal microvascular abnormalities associated with hypertension/sclerosis in the atherosclerosis risk in communities study. Ophthalmology 1999;106:2269–80.

[5] Nakagawa T, Suzuki T, Hayashi Y, Mizukusa Y, Hatanaka Y, Ishida K, et al. Quantitative depth analysis of optic nerve head using stereo retinal fundus image pair. J Biomed Opt 2008;13, 064026-1–10.
[6] Staal JJ, Abramoff MD, Niemeijer M, Viergever MA, van Ginneken B. Ridge based vessel segmentation in color images of the retina. IEEE Trans Med Imaging 2004;23:501–9.
[7] http://www.isi.uu.nl/Research/Database/DRIVE/.
[8] Gao XW, Bharath A, Stanton A, Hughes A, Chapman N, Thom S. Quantification and characterization of arteries in retinal images. Comput Methods Programs Biomed 2000;63:133–46.
[9] Pedersen L, Grunkin M, Ersboll B, Madsen K, Larsen M, Christoffersen N, et al. Quantitative measurement of changes in retinal vessel diameter in ocular fundus images. Pattern Recognit Lett 2000;21:1215–23.
[10] Wong TY, Knudtson MD, Klein R, Klein BEK, Meuer SM, Hubbard LD. Computer-assisted measurement of retinal vessel diameters in the Beaver Dam Eye Study: methodology, correlation between eyes, and effect of refractive errors. Ophthalmology 2004;111:1183–90.
[11] Pakter HM, Ferlin E, Fuchs SC, Maestri MK, Moraes RS, Nunes G, et al. Measuring arteriolar-to-venous ratio in retinal photography of patients with hypertension; development and application of a new semi-automated method. Am J Hypertens 2005;18:417–21.
[12] Tramontan L, Grisan E, Ruggeri A. An improved system for the automatic estimation of the arteriolar-to-venular diameter ratio (AVR) in retinal images. In: Conf Proc IEEE Eng Med Biol Soc. 2008. p. 3550–3.
[13] Tramontan L, Ruggeri A. Computer estimation of the AVR parameter in diabetic retinopathy. IFMBE Proc 2009;25(XI):141–4.
[14] Nam HS, Hwang JM, Chung H, Seo JM. Automated measurement of retinal vessel diameters on digital fundus photographs. IFMBE Proc 2009;25(XI):277–80.
[15] Niemeijer M, van Ginneken B, Abramoff MD. Automatic determination of the artery–vein ratio in retinal fundus images. Proc SPIE 2010;7624, 76240I-1-8.
[16] Rockett PI. An improved rotation-invariant thinning algorithm. IEEE Trans Pattern Anal Mach Intell 2005;27(10):1671–4.
[17] Muramatsu C, Hatanaka Y, Iwase T, Hara T, Fujita H. Automated detection and classification of major retinal vessels for determination of diameter ratio of arteries and veins. Proc SPIE 2010;7624, 76240J-1–8.
[18] Muramatsu C, Nakagawa T, Sawada A, Hatanaka Y, Hara T, Yamamoto T, et al. Automated segmentation of optic disc region on retinal fundus photographs: comparison of contour modeling and pixel classification methods. Comput Methods Programs Biomed 2011;101:23–32.
[19] Tan NM, Liu J, Wong DWK, Lim JH, Li H, Patil SB, et al. Automatic detection of left and right eye in retinal fundus images. ICBME Proc 2009;23:610–4.